Investigating the Influence of Zircaloy-4 Grain Orientation on Oxide Corrosion Films Formed in an Autoclave Environment

Gene A. Lucadamo[1] and Jason A. Gruber[1]

1. Naval Nuclear Laboratory, Core Materials, Manufacturing, and Irradiations, West Mifflin, PA USA.

Early studies of the effect of metal grain orientation on Zr oxidation involved single crystals of pure Zr [1, 2]. While single crystals provided important insight into oxidation behavior as a function of orientation, specimens can be difficult to prepare limiting the amount of data that can be obtained. Also, the behavior of isolated orientations differs from that of a polycrystalline alloy since the potential influence of neighboring grains and second phase precipitates on oxidation are absent. To address some of these limitations, EBSD analysis has been successfully employed in several recent studies of the effects of grain orientation on Zr oxidation [3, 4].

This work combined scanning electron microscopy (SEM), focused ion beam (FIB), and electron backscatter diffraction (EBSD) techniques to characterize oxide films and the crystal orientation of the underlying Zircaloy-4 grains. The oxide films examined were formed during exposure at 360°C in water and varied from 2-4 μm thick, depending on the specimen type and position along the metal-oxide interface. Particular attention was given to the influence of neighboring grains on the local oxide thickness and microstructure as observed from cross-section images. Further, the orientation data was used to construct a correlation based on the angular deviation from the basal plane normal using the normalized oxide thicknesses for several low-index orientations.

Two different specimens of Zircaloy-4 were investigated: one had been processed in the alpha (hcp) phase field and exhibited an equiaxed microstructure, while the other was annealed above the hcp-bcc transition temperature and cooled producing a Widmanstätten microstructure. Figure 1a is an inverse pole figure plot that displays individual grain normals with respect to the surface exposed to the water along with their measured oxide thickness, which have been normalized to facilitate comparisons between the two specimen types. The shading of each point in the IPF corresponds to the thickness of the oxide with the darker points having a thicker oxide film. The metal grains with a surface normal closest to the basal pole <0001> tended to have the thickest oxide, consistent with published reports [1-4]. Figure 1b is a proposed correlation constructed by plotting the film thickness from several grains near low-index orientations.

Figure 2 shows an example where two grains with similar orientations have a different oxide thickness depending on adjacent grains. The orientation map and images on the left show grains that have been identified as having a fast growing orientation and the resulting oxide of the middle grain is thicker than the case shown on the right. While limited to data obtained from a cross-section, the right image shows the grain has a thinner oxide and is greater in size than compared to the image on the left and hence, hypothesized to be less influenced by its neighbors. The differences in corrosion rate as a result of orientation differences in metal grains might also help to explain the periodic formation of lateral cracks in Zr-oxide films and the corresponding influence of these cracks on the overall measured corrosion rate. Addressing of the influence of metal grain orientation on oxidation rate could eventually assist in the development of improved mechanistic models of the corrosion kinetics in Zr-alloys [5].

References:

[1] J Pemsler, J. Electrochem. Soc. **105** (1958) p. 315.

[2] AE Bibb and JR Fascia, Trans. Met. Soc. AIME, **230** (1964) p. 415.

[3] BX Zhou, et al., J. ASTM. Intl. **8** (2011) p. 621.

[4] Y Dong, AT Motta, EA Marquis, Microsc. Microanal. **22** (Suppl. 3) (2016) p. 1496.

[5] The authors thank Drs. R Bajaj, KR Anderson, WH Howland, HM Miller III, and JR Seidensticker for helpful discussions. The authors also thank Dr. JE Ledonne, Dr. JK Heuer and JS Lawrence for assisting with specimen preparation and GA Hoffman for performing the EBSD acquisitions.
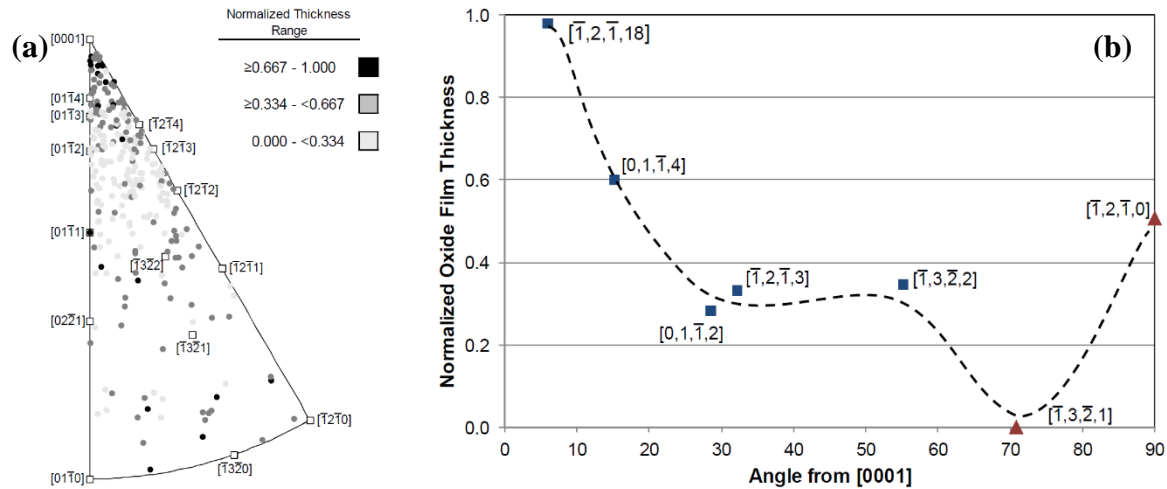
Figure 1. (a) Inverse pole figure (IPF) constructed using the combined EBSD data from the alpha-annealed specimen and beta-quenched specimen. Each point is from a different grain and the gray level corresponds to the normalized thickness of the oxide film. (b) Correlation of oxide thickness with basal pole inclination constructed from data taken from grains having a low-index surface normal. Line is drawn to guide the eye.
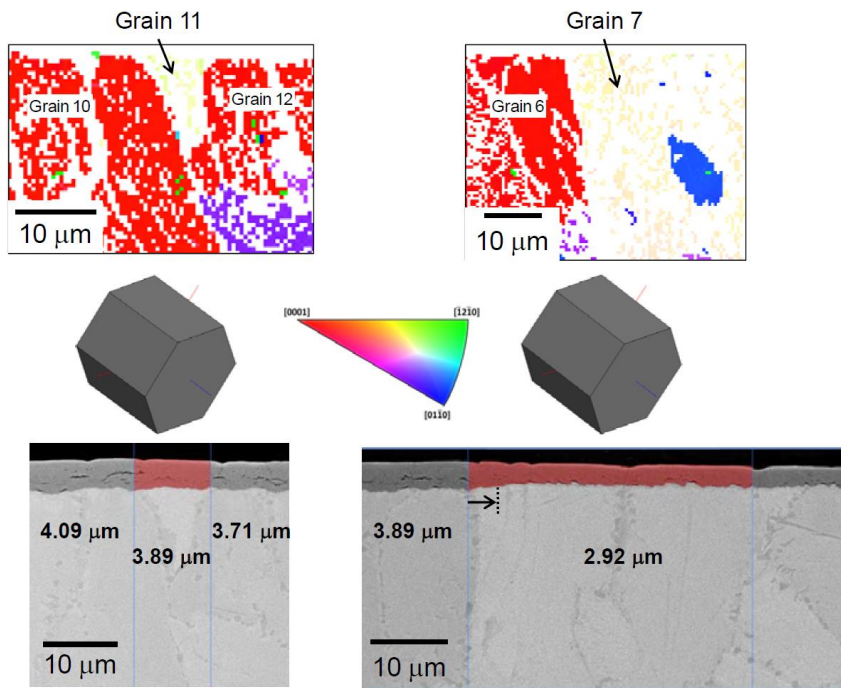
Figure 2. EBSD maps, schematic crystal orientations of the arrowed grains, and backscatter SEM images superimposed with the oxide thickness measurements. Grains 11 and 7 (arrowed) have similar orientations, but the average oxide thickness on grain 11 is greater than the oxide on grain 7. The thicker oxide on grain 11 is hypothesized to result from the influence of the neighboring grains on the oxidation kinetics. Arrow in the lower right SEM image marks the approximate extent of growth enhancement of grain 6 into grain 7.